Advances in Geo-Energy Research

Vol. 19, No. 1, p. 43-57, 2025

Original article

On the mobility reduction factor for the quantification of foam strength in porous media

Gabriel Brandão de Miranda[1,2], Grigori Chapiro[1,3], Rodrigo Weber dos Santos[1,2], Bernardo Martins Rocha[1,2]*

[1]*Computational Modeling Program, Federal University of Juiz de Fora, Juiz de Fora 36036-900 , Brazil*

[2]*Computer Science Department, Federal University of Juiz de Fora, Juiz de Fora 36036-900, Brazil*

[3]*Mathematics Department, Federal University of Juiz de Fora, Juiz de Fora 36036-900, Brazil*

Keywords:
Mobility reduction factor
foam flow
relative permeability
parameter estimation
porous media

Cited as:
de Miranda, G. B., Chapiro, G., dos Santos, R. W., Rocha, B. M. On the mobility reduction factor for the quantification of foam strength in porous media. Advances in Geo-Energy Research, 2025, 19(1): 43-57.
https://doi.org/10.46690/ager.2026.01.04

Abstract:
Foam effects in multiphase flow are commonly modeled as a mobility reduction factor that scales gas mobility. Conventional parameter estimation relies on prior relative permeability functions, introducing epistemic uncertainties that propagate to foam characterization. In this work, an alternative mobility reduction factor formulation expressed solely in terms of pressure drop measurements is derived, eliminating the need for relative permeability assumptions and directly aligning with the modeling hypothesis of gas-only mobility reduction. The approach is evaluated using synthetic foam-quality scan datasets at multiple surfactant concentrations. Profile likelihood analysis shows that the proposed formulation preserves parameter identifiability relative to conventional methods based on apparent viscosity. Robustness is assessed under both correct and misspecified relative permeability models, with the Lomeland-Ebeltoft-Thomas formulation used for data generation and Brooks-Corey curves for parameter estimation. Systematic sampling of relative permeability parameters further demonstrates that, even when the model structure is correct, the proposed mobility reduction factor reduces estimation errors by confining uncertainties to the foam component only. These results establish the new mobility reduction factor definition as a reliable and practical metric for quantifying foam strength in laboratory experiments and for improving parameter estimation in implicit-texture models.

1. Introduction

Subsurface engineering processes that rely on gas injection may face effectiveness issues with the gas phase high mobility. The mobility contrast with resident liquids triggers viscous fingering and gravity override, which in turn yield early breakthrough and poor sweep efficiency. Rock heterogeneity further channels flow through high-permeability pathways, leaving low-permeability zones unswept (Lake, 1988; Shafiei et al., 2024). Foam, a liquid phase trapping dispersed gas stabilized by surfactant, provides a mechanism to mitigate these effects (Tripathi et al., 2024; Wang et al., 2025). It replaces continuous gas with discontinuous bubbles, providing mobility control to divert gas into previously bypassed zones, enhancing volumetric sweep efficiency, and ultimately improving the performance of subsurface operations (Kovscek and Radke, 1994).

Predicting foam behavior at the core scale is critical for transferring laboratory insights to the field (Ma et al., 2015). Numerical simulators such as CMG-STARS (by Computational Modeling Group) represent foam effects through a mobility reduction factor (MRF) that multiplies down gas mobility. In principle, this aligns with the widely accepted view that foam mainly suppresses gas flow (Bernard and Jacobs,

Yandy Scientific Press

*Corresponding author.
E-mail address: gabriel.miranda@estudante.ufjf.br (G. B. de Miranda); grigori.chapiro@ufjf.br (G. Chapiro); rodrigo.weber@ufjf.br (R. W. dos Santos); bernardomartinsrocha@ufjf.br (B. M. Rocha).

Received October 28, 2025; revised November 26, 2025; accepted December 19, 2025; available online December 22, 2025.

1965; Kovscek and Radke, 1994; Rossen, 1996; Eftekhari and Farajzadeh, 2017). In this context, foam strength refers to the foam ability to reduce gas mobility, a property significantly influenced by foam quality (the gas fraction in the injected fluid). Experimentally (Osterloh and Jante, 1992; Rossen, 1996), foam strength has been observed to increase with foam quality, but it begins to decline at high gas fractions due to dry-out effects. Foam strength is usually assessed through apparent viscosity, which correlates with pressure drop and is affected by both gas and liquid phases (Farajzadeh et al., 2015; Eftekhari and Farajzadeh, 2017). However, experimental formulations of MRF do not clearly distinguish the reduction in gas-phase mobility, which makes it inconsistent with the modeling assumption of gas-only mobility reduction, complicating parameter estimation (Lotfollahi et al., 2016).

Most approaches, therefore, rely on relative permeability functions to disentangle phase contributions (Ma et al., 2014). Yet relative permeability estimation is itself uncertain and strongly affects the identifiability of foam parameters (Zeng et al., 2016; Cavalcante Filho et al., 2017; de Miranda et al., 2024; Ribeiro et al., 2024). This creates a two-layer uncertainty source: First in relative permeability, then in foam characterization.

In this work, an alternative formulation of the MRF that isolates the gas-phase contribution directly is proposed, eliminating the need for relative permeability functions. The method is derived algebraically from the steady-state experimental definition of MRF, producing a gas-specific expression consistent with simulator formulations such as CMG-STARS. Then its performance is evaluated for parameter estimation using synthetic foam-quality scans, comparing it against the conventional apparent-viscosity-based objective function. Identifiability and robustness are assessed under both correct and misspecified relative permeability models, highlighting how the proposed definition confines the uncertainty to the foam parameters alone.

2. Mathematical modeling

The foam flow in porous media can be modeled by a multiphase system with surfactant transport, where phases are assumed to be incompressible and immiscible. The system involves mass conservation for each phase, flow relationships for phase velocities, and transport of surfactant. Phase saturations are denoted by S_α, velocities by u_α, where for the two-phase considered here $\alpha \in \{w, g\}$, and C_s represents the aqueous surfactant concentration (Zavala et al., 2024). These governing equations are simplified under the conditions of steady-state laboratory experiments, where constant inlet fluxes, pressures, and surfactant concentration are assumed. This reduces the mass conservation and transport equations to algebraic expressions (de Miranda et al., 2022; Valdez et al., 2022b). The homogeneity hypothesis results in spatial invariance of saturations and concentrations, yielding a constant pressure drop ΔP, water saturation, and surfactant concentration (Ma et al., 2013; Eftekhari and Farajzadeh, 2017; Kahrobaei and Farajzadeh, 2019).

The fractional flow f_α of a phase α is defined as the ratio of the phase velocity to the total velocity of all phases flowing through the porous medium:

$$f_\alpha = \frac{u_\alpha}{u_T}, \quad u_T = \sum_\alpha u_\alpha \tag{1}$$

where u_T is the total superficial velocity in the flow direction. At steady-state conditions in experimental settings, the apparent viscosity μ_{app} of the system can be calculated as follows:

$$\mu_{app} = \lambda_T^{-1} = \frac{K}{u_T}\frac{\Delta p}{L} \tag{2}$$

where λ_T is the total mobility, K is the absolute permeability of the domain, Δp is the pressure difference, and L is the length of the core. At steady-state, the fractional flow of each phase can also be expressed mathematically as the ratio of its mobility to the total mobility, that is:

$$f_\alpha = \frac{\lambda_\alpha}{\lambda_T} \tag{3}$$

where the phase mobility is given by $\lambda_\alpha = k_{r\alpha}/\mu_\alpha$, and depends on relative permeability $k_{r\alpha}$ and viscosity μ_α of phase α.

2.1 Relative permeability

Relative permeabilities are usually described either by the Brooks-Corey (Brooks and Corey, 1964) or Lomeland-Ebeltoft-Thomas (LET) models (Lomeland et al., 2005). Without considering foam effects, the Brooks-Corey form for water-gas flow is given by:

$$k_{rw}^{Corey} = k_{rw}^0 s_w^{n_w}, \qquad k_{rg}^{Corey} = k_{rg}^0 (1 - s_w)^{n_g} \tag{4}$$

with the normalized water saturation defined by:

$$s_w = \frac{S_w - S_{wc}}{1 - S_{wc} - S_{gr}} \tag{5}$$

where n_w and n_g are the Corey exponents.

The LET functions for relative permeability (Lomeland et al., 2005), which offer more flexibility to describe multiphase flow, are defined as:

$$k_{rw}^{\mathrm{LET}} = k_{rw}^0 \frac{s_w^{L_w}}{s_w^{L_w} + E_w (1 - s_w)^{T_w}} \tag{6}$$

$$k_{rg}^{\mathrm{LET}} = k_{rg}^0 \frac{(1 - s_w)^{L_g}}{(1 - s_w)^{L_g} + E_g s_w^{T_g}} \tag{7}$$

where L_w, L_g control the lower part of the curve, E_w, E_g determine transition curvature, T_w, T_g characterize upper part of the curve, and S_{wc} and S_{gr} denote connate water and residual gas saturations. In general, the LET correlation functions for relative permeability provide a better description of the data (Berg et al., 2021).

2.2 Foam model

The implicit-texture formulation implemented in CMG-STARS (STARS, 2017) represents foam effects through a MRF term applied to reduce the gas phase mobility. For water-gas systems, the apparent viscosity is expressed as:

$$\mu_{app} = \left(\lambda_w + \frac{\lambda_g}{\text{MRF}}\right)^{-1} = \left(\frac{k_{rw}}{\mu_w} + \frac{k_{rg}}{\mu_g \text{MRF}}\right)^{-1} \tag{8}$$

while the MRF of the foam apparent viscosity model (STARS) is given by:

$$\text{MRF} = 1 + fmmob \prod_i F_i \tag{9}$$

where F_i represent dimensionless functions capturing various foam destabilization mechanisms. This work considers two primary effects: The dry-out function F_{dry} accounting for foam coalescence at low water saturations, and the surfactant function F_{surf} representing concentration-dependent foam stability.

The dry-out function takes the form:

$$F_{dry}(S_w) = \frac{1}{2} + \frac{\arctan[epdry(S_w - fmdry)]}{\pi} \tag{10}$$

where *fmdry* represents an approximation for the critical water saturation below which foam becomes unstable and collapses, and *epdry* controls the sharpness of the transition from the low- to high-quality regimes (Osterloh and Jante, 1992). The surfactant concentration effect is modeled as:

$$F_{surf}(C_s) = \begin{cases} \left(\dfrac{C_s}{fmsurf}\right)^{epsurf} & \text{if } C_s < fmsurf \\ 1 & \text{otherwise} \end{cases} \tag{11}$$

where *fmsurf* denotes the reference surfactant concentration and *epsurf* determines the sensitivity of foam strength to concentration changes.

Estimation of the parameters for this model relies on steady-state core flooding experiments conducted at various foam qualities and surfactant concentrations. The primary observable is the relationship between apparent viscosity and injected gas fraction at constant total velocity. As foam quality increases, the apparent viscosity initially rises due to foam generation, then decreases beyond a transition quality f_g^* corresponding to the onset of dry-out conditions. The reference MRF *fmmob* scales the overall foam strength and is determined through history matching of experimental pressure drop and saturation data (Ma et al., 2013).

2.3 The MRF expression

Since the first application of foam for gas mobility control (Bond and Holbrook, 1956), the quantification of its mobility-reduction capability has evolved from empirical correlations toward a mechanistic understanding (Ma et al., 2015). While the assumption of foam reducing solely gas-phase mobility prevails (Bernard and Jacobs, 1965; Eftekhari and Farajzadeh, 2017), modeling approaches in the literature have linked the experimentally measured ratio of pressure drop with and without foam (Mohammadi et al., 1995; Chang and Grigg, 1996; Ma et al., 2015). Typically, the MRF is computed using the following expression:

$$\frac{\Delta P_{foam}}{\Delta P_{ref}} \tag{12}$$

to characterize foam. However, even approaches assuming that foam affects solely gas-phase mobility may be misled by inconsistencies between this modeling assumption and the classical definition of such ratios during parameter estimation (Vieira et al., 2024; Hematpur et al., 2025).

According to Rosman and Kam (2009), the MRF is determined from the pressure drop ratio between the foam and no-foam conditions in the same rock sample at identical saturation states. In the literature, however, the no-foam pressure drop ΔP_{ref} has been defined in different ways: Continuous brine injection (Simjoo et al., 2013; Jia et al., 2024), continuous gas injection (Bello et al., 2023), or water-gas co-injection (Sri-Hanamertani et al., 2021; AlYousef et al., 2023). Each condition yields distinct quantities associated with MRF, hindering direct comparison of experimental results and complicating parameter estimation in foam simulators.

2.4 Current parameters estimation procedures

In a steady-state scenario, the relative permeability for any chosen model can be written in terms of experimentally measurable quantities:

$$k_{r\alpha} = \frac{\mu_\alpha f_\alpha}{\mu_{app}} \tag{13}$$

A significant assumption among the methods for foam parameter fitting relying on apparent viscosity measurements (Eq. (8)) is that the relative permeability functions are known prior to analysis (Ma et al., 2013; Eftekhari and Farajzadeh, 2017; Vicard et al., 2022; Valdez et al., 2022b). However, its accuracy relies on the adequacy of the relative permeability model and the quality of the data used for parameter fitting; uncertainties in either the model or its parameters at this stage inevitably propagate into the foam parameter estimates.

Procedures for foam parameter estimation relying on steady-state data from a foam-quality scan or flow-rate scan, without monitoring water saturation experimentally, generally assume that the relative permeabilities are described by the modified Brooks-Corey model (Brooks and Corey, 1964). The experiments provide data points in the form of (f_g^i, μ_{app}^i). To evaluate the STARS model for parameter estimation, however, the corresponding water saturation must be determined for each given pair (f_g, μ_{app}). Therefore, if the Brooks-Corey form is assumed, the corresponding water saturation can be analytically inverted, as proposed by Farajzadeh et al. (2015) and Eftekhari and Farajzadeh (2017), as follows:

$$S_w = \left[\frac{(1-f_g)\mu_w}{k_{rw}^0 \mu_{app}}\right]^{1/n_w} (1 - S_{wc} - S_{gr}) + S_{wc} \tag{14}$$

Once S_w is obtained for each pair (f_g, μ_{app}), STARS can be computed, since it depends on S_w through $F_{dry}(S_w)$ (Eqs. (8)-(10)). Since S_w estimation from apparent viscosity data relies on assumed relative permeability functions (Eq. (14)), uncertainties in these functions further propagate to parameter estimation.

The LET relative permeability model described in Eq. (7), unlike the Brooks-Corey model, cannot be analytically inverted for saturation, requiring numerical methods for this inversion. Consequently, its application with the STARS foam flow model has been limited. In the following, a new expression to quantify the MRF is introduced, enabling the

estimation of foam parameters without prior knowledge of, or assumptions about, the relative permeabilities.

2.5 Derivation of a new MRF expression

In this work, an alternative expression connecting experimental measurements of pressure drop to the MRF term used in foam models is derived from the formula given in Eq. (12) following the experimental requirements defined by Rosman and Kam (2009). The present approach contributes to establishing a quantity that does not depend on relative permeability for foam characterization. This is because the empirical effects in the MRF term depend directly on observable variables and do not require knowledge of modeling phase mobilities.

Starting from a steady-state flow at the same saturation levels, the pressure drop ratio between the foam and no-foam cases is analogous to the ratio between the total mobilities, which can be expressed as:

$$\frac{\Delta P_{foam}}{\Delta P_{ref}} = \frac{\dfrac{u_T L}{K}\mu_{app}^{foam}}{\dfrac{u_T L}{K}\mu_{app}^{ref}} = \frac{\mu_{app}^{foam}}{\mu_{app}^{ref}} = \frac{\lambda_T^{ref}}{\lambda_T^{foam}} = \frac{\lambda_l + \lambda_g}{\lambda_l + \dfrac{\lambda_g}{\mathrm{MRF}}} \tag{15}$$

where λ_l represents liquid phase mobility (water or combined water-oil in three-phase systems). Next, rearranging to isolate the foam-induced pressure increment yields the following expression:

$$\begin{aligned}\frac{\Delta P_{foam}}{\Delta P_{ref}} - 1 &= \frac{\lambda_l + \lambda_g}{\lambda_l + \dfrac{\lambda_g}{\mathrm{MRF}}} - 1 \\ &= \frac{\lambda_l + \lambda_g - \left(\lambda_l + \dfrac{\lambda_g}{\mathrm{MRF}}\right)}{\lambda_l + \dfrac{\lambda_g}{\mathrm{MRF}}} \\ &= \frac{\dfrac{\lambda_g}{\mathrm{MRF}}(\mathrm{MRF} - 1)}{\lambda_l + \dfrac{\lambda_g}{\mathrm{MRF}}}\end{aligned} \tag{16}$$

Normalizing by the steady-state form of the gas fractional flow f_g in presence of foam (Eq. (3)) isolates the contribution to gas-phase:

$$\mathrm{MRF} = 1 + \frac{\Delta P_{foam} - \Delta P_{ref}}{f_g \Delta P_{ref}} = \frac{\Delta P_{foam} - (1 - f_g)\Delta P_{ref}}{f_g \Delta P_{ref}} \tag{17}$$

The MRF term is designed in implicit-texture foam models by adding a unitary regularization term to the part modeling the foam effects in reducing gas mobility, as shown in Eq. (8) (right), ensuring that gas mobility returns to its original state when foam effects vanish. Indeed, if $\Delta P_{foam} = \Delta P_{ref}$ in Eq. (17), then $\mathrm{MRF} = 1$.

Note that Eq. (17) can also be written as:

$$\mathrm{MRF} = \frac{\Delta P_{foam} - f_l \Delta P_{ref}}{f_g \Delta P_{ref}} \tag{18}$$

which clearly and correctly defines MRF. The numerator subtracts the liquid contribution of the reference pressure drop, $f_l \Delta P_{ref}$, from the total foam pressure drop, isolating the portion attributable to the gas phase under foam. The denominator, $f_g \Delta P_{ref}$, is the gas contribution of the reference pressure drop. Thus, MRF quantifies the foam-induced amplification of gas-phase resistance relative to its baseline, without requiring relative-permeability curves.

Observe that, if $f_l \Delta P_{ref}$ were replaced by $f_l \Delta P_{foam}$, Eq. (18) would reduce to the simple ratio $\Delta P_{foam}/\Delta P_{ref}$, thereby losing the gas-specific normalization. In that case, the MRF definition would implicitly incorporate changes related to the liquid phase, while the objective of MRF is to isolate the effect of foam on the gas phase only. Therefore, the subtraction must involve the liquid contribution of the reference case, ensuring that MRF remains a gas-specific measure of foam strength.

Fig. 1 illustrates the alignment between the proposed MRF expression (dots) and the one computed with the CMG-STARS equation (solid line), in comparison to the classical MRF definition (crosses), $\Delta P_{foam}/\Delta P_{ref}$, using noisy datasets for foam and no-foam experiments. A quantitative analysis was also performed to complement the visual inspection. Since the MRF values span several orders of magnitude, the evaluation employed the Mean Absolute Percentage Error (MAPE) as a scale-invariant metric. The classical MRF definition exhibited substantial deviations (average MAPE ≈ 1.75), whereas the proposed formulation demonstrated high accuracy across all scenarios (average MAPE ≈ 0.007).

It is observed that for low f_g values, the classic definition drastically underestimates the correct value of MRF, since f_l is high. Because it normalizes by the total (liquid+gas) reference drop rather than the gas contribution, the large liquid contribution in the denominator reduces the foam-induced gas resistance. Indeed, since:

$$\frac{\Delta P_{foam}}{\Delta P_{ref}} = \frac{\lambda_l + \lambda_g}{\lambda_l + \dfrac{\lambda_g}{\mathrm{MRF}}} = \frac{1}{1 - f_g + \dfrac{f_g}{\mathrm{MRF}}} \tag{19}$$

in the liquid-dominated limit $f_g \to 0$, this ratio tends to unity regardless of the actual value of MRF. Therefore, $\Delta P_{foam}/\Delta P_{ref}$ systematically underestimates the correct MRF when f_g is small. On the other hand, the novel estimation of MRF follows the true values. This comparison demonstrates that the proposed expression aligns more closely with the model formulation, supporting its use for direct parameter estimation based on only pressure drop measurements.

3. Dataset and parameter estimation approach

Synthetic datasets were generated using the implicit-texture foam model (Eq. (8)) with known parameter values to focus on the mathematical aspects of parameter estimation and uncertainty quantification approaches. This strategy eliminates experimental uncertainties and model-data mismatch, allowing comparisons to a reference value to understand the fundamental properties of different estimation methods, and has been used extensively in the literature (Berg et al., 2024; de Miranda et al., 2024; Ribeiro et al., 2024).

To generate the dataset, our models and parameters are based on the work of Jones et al. (2016). The foam parameters were derived from their data using steady-state multiphase flow equations with foam effects (Eqs. (1)-(7)). However, to assess robustness against model mismatch, the LET functions are used. To this end, the relative permeabilities reported by

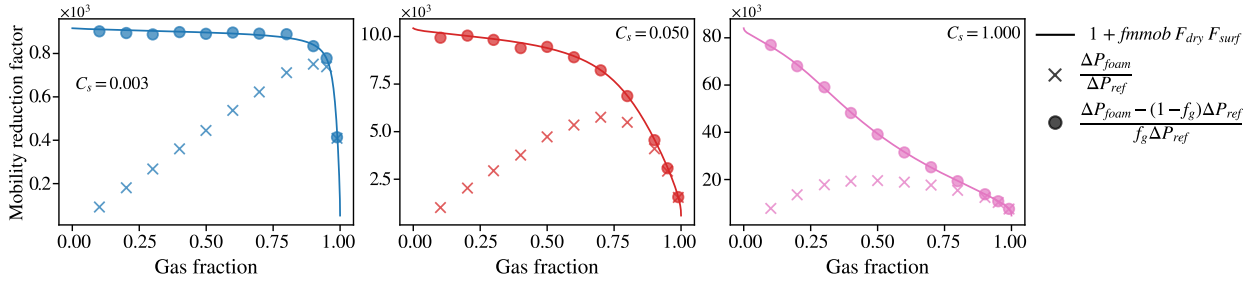

Fig. 1. Comparison of the MRF expression in the CMG-STARS model (solid line) in front of the datasets considering the two formulas, Eq. (12) (cross) and Eq. (17) (dot), over noisy observations for different surfactant concentrations. As the concentration increases, the impact of noise on saturation and pressure drop becomes less significant, improving the precision of the calculations.

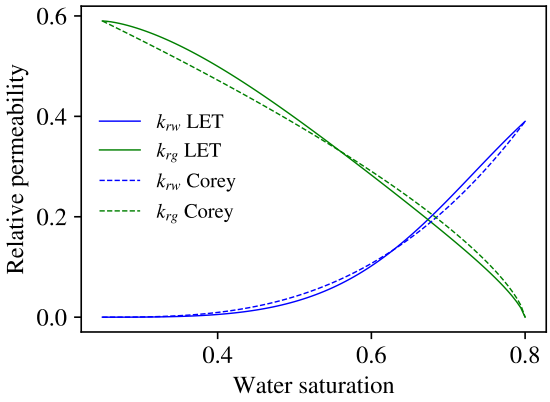

Fig. 2. Comparison of LET (solid lines) and Brooks-Corey (dashed lines) relative permeability functions used in this work.

Jones et al. (2016) are approximated, which are Brooks-Corey based, using the LET relative permeabilities. Fig. 2 shows the LET relative permeability functions used in this work (solid lines), which were based on data from the Brooks-Corey representation of Jones et al. (2016). The parameters of the LET functions are reported in Table 1, along the original Corey exponents ($n_w = 2.86$, $n_g = 0.7$) from Jones et al. (2016). It is important to note that the LET function can reproduce the shape of the Brooks-Corey function, whereas the converse is not necessarily true. This flexibility gives the LET formulation a broader applicability and makes it better suited for representing diverse relative permeability behaviors (Valdez et al., 2020; Berg et al., 2021).

With the set of parameters reported in Table 1, the dataset presented in Fig. 3 spanned surfactant concentrations of 0, 0.003, 0.01, 0.03, 0.05, 0.1, 0.5, and 1.0 wt%. The zero-concentration case provides the reference conditions required for MRF calculation using Eq. (17), conducted at high gas fractions to achieve high gas saturations, similar to those observed in the presence of foam. Simulations include foam qualities from 0.1 to 0.99, generating pressure drop and saturation data where true parameter values are known exactly. A 10% Gaussian noise is added to the apparent viscosity and saturation values to simulate uncertainty inherent in experimental measurements (Berg et al., 2024). The original dataset

Table 1. Parameter values used for synthetic generation based on Jones et al. (2016).

Type	Parameter	value
Foam	$fmmob$ (-)	84,916
	$fmdry$ (-)	0.334
	$epdry$ (-)	66.7
	$fmsurf$ (-)	0.558
	$epsurf$ (-)	0.865
Relative permeability	k^0_{rw} (-)	0.39
	S_{wc} (-)	0.25
	L_w (-)	3.0
	E_w (-)	2.0
	T_w (-)	1.0
	k^0_{rg} (-)	0.59
	S_{gr} (-)	0.2
	L_g (-)	0.75
	E_g (-)	1.0
	T_g (-)	1.5
Fluid/rock properties	u_w (Pa·s)	1.0×10^{-3}
	u_g (Pa·s)	1.805×10^{-5}
	u_t (m/s)	2.4×10^{-5}
	σ (N/m)	0.0291
	ϕ (-)	0.23

from Jones et al. (2016) and the synthetic dataset are presented in the left and right panels of Fig. 3.

The steady-state foam corefloods from Jones et al. (2016) were conducted on Bentheimer sandstone cores at 60 °C and 20 bar back-pressure. Nitrogen and an AOS surfactant solution were co-injected at a constant superficial velocity of 2.4×10^{-5} m/s to generate foam, while pressure drop was measured. The differences between the original dataset and model-generated data arise from model limitations that do not fully capture the experimentally observed behavior.

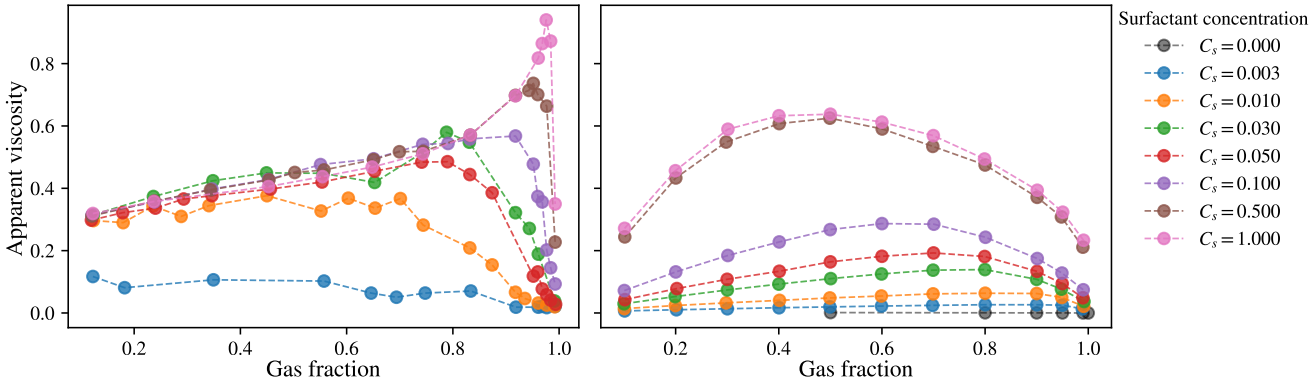

Fig. 3. Apparent viscosity vs foam quality for different surfactant concentrations. Left: The original data from Jones et al. (2016) data. Right: The synthetic data at the same surfactant concentrations, plus a no surfactant experiment, that is, without foam, used as a reference for MRF calculation.

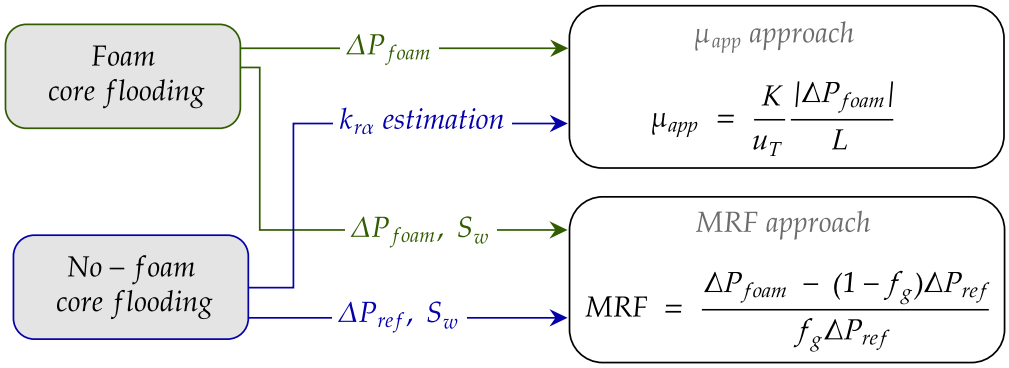

Fig. 4. Workflow comparison for foam parameter estimation. The MRF approach uses reference experiments at matching saturations to directly calculate MRF. The Apparent Viscosity approach requires a separate relative permeability characterization to model apparent viscosity. Both methods optimize for the same foam model parameters using different objective functions.

Therefore, from this point onward, the dataset generated with the parameters estimated by Jones et al. (2016) is used. Based on these data, two distinct datasets were constructed. The first dataset provides direct measurements of apparent viscosity (μ_{app}) in relation to foam quality (f_g). The second dataset contains calculated MRF values derived from pressure drop measurements based on the proposed Eq. (17); the data are presented for three selected surfactant concentrations in Fig. 1.

4. Methods

The two parameter estimation approaches evaluated in this work are illustrated in Fig. 4, which highlights the fundamental differences in their workflows and data requirements. The apparent viscosity approach (highlighted in blue) requires previous knowledge of the relative permeability functions and the pressure drop with foam. In contrast, the proposed MRF approach of this work (highlighted in green) relies solely on pressure experimental data with and without foam, and no information about the relative permeabilities is required.

4.1 Foam parameter estimation

In this section, the objective functions employed for foam parameter estimation are described. Two alternatives are considered: One based on apparent viscosity (Eq. (8)) and another based on the MRF proposed in this work (see Eq. (17)). Both functions represent the normalized sum of squared deviations between model predictions and experimental observations.

The accuracy of the methods for estimating foam parameters using apparent viscosity observations also depends on the adequacy of the assumed relative permeability model and its estimated parameters. A structural mismatch between the assumed $k_{r\alpha}$ functions and the true flow behavior or parametric uncertainties propagates into foam parameter estimates (Ma et al., 2013; Eftekhari and Farajzadeh, 2017; Valdez et al., 2022b; Vicard et al., 2022).

In the following, the apparent viscosity-based and MRF-based parameter estimation approaches are formulated as optimization problems.

Apparent viscosity approach: Given the observed apparent viscosity μ_{app}^{obs}, and the relative permeability parameters κ to evaluate apparent viscosity model μ_{app}^{model} using Eq. (8), find foam parameters θ that minimizes

$$\chi^2_{\mu_{app}}(\theta;\kappa) = \sum_i \left[\frac{\mu_{app,i}^{model}(\theta;\kappa) - \mu_{app,i}^{obs}}{\max(\mu_{app}^{obs})}\right]^2 \tag{20}$$

It is important to note that procedures lacking saturation monitoring necessitate the estimation of S_w from (f_g, μ_{app}), as

Table 2. Parameter bounds used in differential evolution optimization.

Parameter	Lower bound	Upper bound
fmmob	10^3	10^7
fmdry	S_{wc}	$1.0 - S_{gr}$
epdry	10^1	10^5
fmsurf	10^{-2}	2.0
epsurf	10^{-2}	5×10^1

detailed in Eq. (14). This issue may become more significant for complex models that do not permit analytical inversion, as Corey-Brooks (Eq. (14)).

MRF approach: Given the observed MRF MRF^{obs} (Eq. (17)), find foam parameters θ that minimizes:

$$\chi^2_{\mathrm{MRF}}(\theta) = \sum_i \left[\frac{\mathrm{MRF}_i^{model}(\theta) - \mathrm{MRF}_i^{obs}}{\max(\mathrm{MRF}^{obs})} \right]^2 \tag{21}$$

A key advantage of the MRF approach is that it estimates foam parameters without requiring prior knowledge of relative permeability functions.

Both optimization problems were carried out using the differential evolution (DE) method, a population-based stochastic search algorithm (Storn and Price, 1997; Price, 2013), and relied on the following settings across all scenarios: A population size of 500 individuals for the DE method evolved over 500 generations within the parameter space limited by physical constraints presented in Table 2.

4.2 Profile likelihood analysis

Parameter identifiability is a fundamental aspect to support reliable model calibration. Profile likelihood (PL) analysis is a technique for assessing practical and structural identifiability by examining the objective-function topology in the vicinity of optimal values (Raue et al., 2009), thereby highlighting correlation structures and potential ambiguities in parameter estimation.

The PL method involves fixing each parameter of interest at specified values while optimizing the remaining parameters to minimize the objective function. To this end, in this work, each parameter was systematically varied within ±50% of its reference value, generating 200 evaluation points per profile. At each fixed parameter value, 20 independent optimization runs of the DE method were performed with randomized initial populations to ensure robust convergence and capture potential local minima.

Three distinct scenarios were examined to evaluate the influence of relative permeability characterization on foam parameter identifiability:

1) The first scenario represents ideal conditions, where the apparent viscosity objective function presented in Eq. (20) is minimized using the ground-truth relative permeability functions. This baseline establishes the intrinsic identifiability limits of foam parameters under perfect knowledge of multiphase flow properties.
2) The second scenario employs the apparent viscosity objective function again, Eq. (20). However, it adopts a misspecified relative permeability function, particularly assuming the Brooks-Corey functions instead of the LET functions, illustrated in Fig. 2, the subtle yet critical model discrepancy. It represents the common experimental conditions where relative permeability characterization contains uncertainties in model specification and parameter fitting.
3) The third scenario evaluates the MRF formulation, presented in Eq. (21), which, by construction, eliminates direct dependence on relative permeability functions during optimization.

4.3 Relative permeability uncertainty quantification

Following the establishment of parameter identifiability through profile likelihood analysis, an uncertainty quantification analysis was carried out to assess the robustness of each foam parameter estimation approach. This evaluation analyzes how uncertainties in relative permeability characterization propagate through the parameter estimation process and influence the reliability of the estimated foam parameters.

To evaluate uncertainties, data was generated by sampling the Corey-Brooks relative permeability parameters, $\kappa = \{n_w, n_g, k^0_{rw}, k^0_{rg}\}$, using Latin Hypercube Sampling (Iman and Conover, 1982). The parameters were sampled from Gaussian distributions centered at their ground truth values ($n_w = 2.86$, $n_g = 0.7$, $k^0_{rw} = 0.39$, and $k^0_{rg} = 0.59$) with a ±10% variation, generating 2^{13} parameter sets that span the uncertainty space.

For each sampled relative permeability parameter set, two estimation pathways were evaluated to enable direct comparison between the strategies presented in Fig. 4. The apparent viscosity approach employs the perturbed relative permeability functions in μ_{app} calculations during foam parameter optimization, representing the conventional methodology where relative permeability characterization uncertainties directly affect the estimation process (for further details see Eftekhari and Farajzadeh (2017)).

The MRF approach utilizes the same perturbed relative permeability functions to generate reference pressure drop values ΔP_{ref}, which, combined with foam experiment pressure drops ΔP_{foam}, are used to calculate MRF values according to Eq. (17). Foam parameters are subsequently estimated using just the MRF dataset without relying on relative permeability knowledge functions during optimization. While in the apparent viscosity approach, monitoring water saturation is just an optional step, it assumes a relative permeability function, which introduces epistemic uncertainty. In contrast, the MRF approach does require monitoring saturations but does not make any assumption about the relative permeability.

5. Results

First, the alignment of the proposed MRF expression for characterizing foam experimental data to the STARS foam model is presented. Then, the results of the methods discussed in the preceding section are presented, which were used to

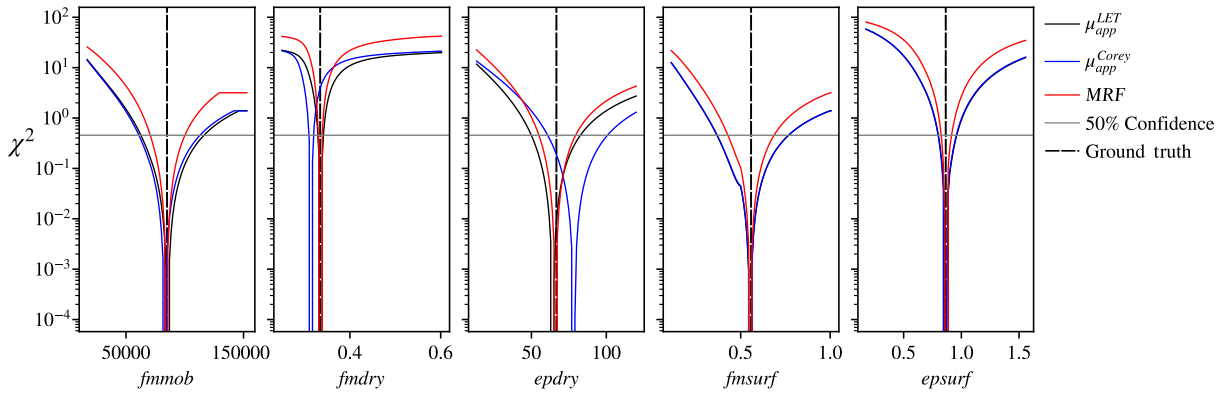

Fig. 5. Profile likelihood analysis for foam parameter estimation under three scenarios: μ_{app}^{LET}: Apparent viscosity objective function assuming the correct relative permeability functions that generated the data (LET); μ_{app}^{Corey}: Apparent viscosity objective function assuming assuming wrong relative permeability functions (Corey); MRF: MRF objective function, no relative permeability assumptions. Vertical lines indicate ground truth parameter values.

Table 3. Parameter estimation comparison between μ_{app} and MRF methods considering LET relative permeability for data generation.

Parameter	Ground truth	Estimate (absolute relative error)		
		μ_{app} w/Corey	μ_{app} w/LET	MRF
fmmob (10^5)	0.849	0.830 (2.24%)	0.854 (0.58%)	0.845 (0.49%)
fmdry (10^{-1})	3.344	3.148 (5.88%)	3.354 (0.30%)	3.345 (0.02%)
epdry (10^1)	6.666	7.846 (17.70%)	6.435 (3.46%)	6.606 (0.90%)
fmsurf (10^{-1})	5.580	5.532 (0.87%)	5.524 (1.00%)	5.540 (0.72%)
epsurf (10^{-1})	8.649	8.648 (0.01%)	8.673 (0.28%)	8.659 (0.12%)

evaluate parameter identifiability and quantify the uncertainty associated with variability in the relative permeability function.

5.1 MRF

The STARS model evaluation is presented in Fig. 1, showing the ground-truth parameters (solid line) compared to the MRF calculated using Eq. (12) (cross) or Eq. (17) (dot) at three selected surfactant concentrations. First, it is evident that the proposed expression for MRF quantification aligns more closely with the data obtained using the STARS foam mathematical model. Moreover, as the surfactant concentration increases and the foam strengthens, the proposed MRF appears to be less sensitive to noise.

5.2 Parameter identifiability

The profile likelihood results are presented in Fig. 5 for three scenarios: apparent viscosity objective function with known relative permeability functions (μ_{app}^{LET}, using the ground truth parameters), apparent viscosity objective function with a mismatch in relative permeability functions (μ_{app}^{Corey}), and MRF objective function (MRF). Each column represents a different profiled parameter. Table 3 presents a quantitative assessment of this analysis, showing the absolute relative errors of the different approaches computed with respect to the ground-truth parameters.

In the first scenario (Fig. 5, solid black line), the profile likelihood exhibits well-defined minima within the confidence threshold of 50% for all foam parameters when using the apparent viscosity approach with correct relative permeability functions (without uncertainty in relative permeability). This confidence threshold defines the range of acceptable parameter estimates that maintain at least half of the maximum likelihood. The formulation that incorporates the MRF into the objective function (Fig. 5, solid red line) also demonstrates close agreement with the ground truth parameters.

The case where noise is introduced in the relative permeability functions to represent difficulties in their estimation significantly impacts the identifiability profiles, as shown in the blue lines in Fig. 5. Notable deviations from the ground truth values occur for *fmdry* and *epdry*, with the objective function minima shifting substantially from their true positions. Although the mismatch in *fmdry* seems small, it is important to recognize that even minor deviations in this parameter can have a substantial effect on model predictions (Valdez et al., 2022a).

The results of the foam parameter estimation are summarized in Table 3 for each approach. The apparent viscosity method produced significant errors, as it incorrectly attributed the relative permeability model (mismatch) to foam effects. In contrast, the MRF approach, being agnostic to the permeability

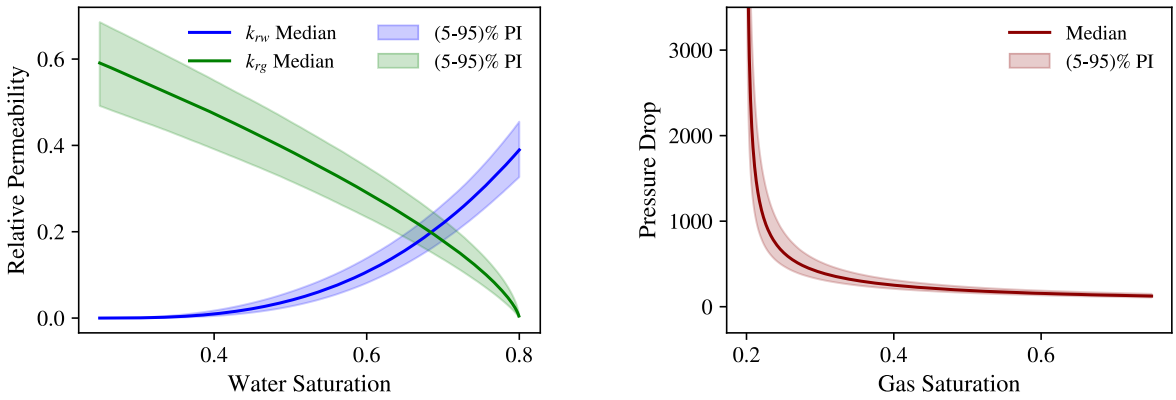

Fig. 6. Propagated uncertainties from relative permeability parameters to the relative permeability functions (left) and to the reference pressure drop (right).

Table 4. Comparison of estimated values from both approaches and their relative error against the ground truth values.

Parameter	Ground truth	Maximum error (relative error)	
		μ_{app} approach	MRF approach
fmmob (10^5)	0.849	0.516 (-39.28%)	0.506 (-40.47%)
fmdry (10^{-1})	3.344	3.977 (18.91%)	3.328 (-0.48%)
epdry (10^1)	6.666	13.810 (107.11%)	6.385 (-4.21%)
fmsurf (10^{-1})	5.580	4.585 (-17.84%)	5.925 (6.18%)
epsurf (10^{-1})	8.649	9.152 (5.82%)	8.837 (2.18%)

model, closely approximated the true foam parameters.

5.3 Uncertainty propagation from relative permeability functions

The uncertainties in the relative permeability parameters κ are propagated to the model outputs, namely the apparent viscosity and the MRF. To evaluate the impact on the estimated parameters, multiple runs of the parameter estimation process were conducted.

First, Fig. 6 (left panel) shows the uncertainties from relative permeability parameters to the relative permeability functions. The right panel of Fig. 6 shows the result of propagating the relative permeability uncertainties to the no-foam reference pressure drop, which is required for the MRF approach.

Next, a set of 2^{13} parameter estimation runs were carried out to provide a statistically robust characterization of bias and variance in estimated foam parameters under uncertainty in relative permeability in order to compare the approaches using μ_{app} or MRF. Table 4 presents a comparison of the maximum error committed when using the two different approaches. The maximum relative errors demonstrate that the MRF approach consistently yields better approximations for the dry-out parameters (*fmdry* and *epdry*). On the other hand, both methods show similar performance for the other parameter estimation. The improved performance of the MRF method observed in Table 4 stems from its theoretical consistency with the gas-only mobility reduction hypothesis. While the μ_{app} approach relies on inversion of relative permeability models to estimate water saturation, the MRF method requires explicit saturation monitoring. This direct measurement of water saturation is especially advantageous for estimating dry-out parameters (*fmdry*, *epdry*), which are strongly connected to water saturation behavior. By eliminating the need for relative permeability inversions and directly measuring the saturation that controls foam dry-out, the MRF approach drastically reduces uncertainty in these critical parameters.

A more detailed analysis of the estimated parameters is presented in Fig. 7 that compares the fitting results of the two approaches in a joint plot of the estimated values θ for sampled relative permeability parameters κ. For all parameters except *fmmob*, the μ_{app} approach produces a wider spread of estimated parameter values than the MRF approach, indicating a greater propagation of uncertainties in these parameters. With respect to Fig. 7, one can also note that the MRF approach for foam parameter estimation reduces the range of estimated parameters, and consequently, the associated uncertainties, particularly for the *epdry* and *fmdry* parameters. This improvement stems from the MRF approach explicitly incorporating information about water saturation.

6. Discussions

6.1 Relative permeability models

The proposed MRF approach, while requiring saturation monitoring, which can be obtained through CT (Simjoo et al.,

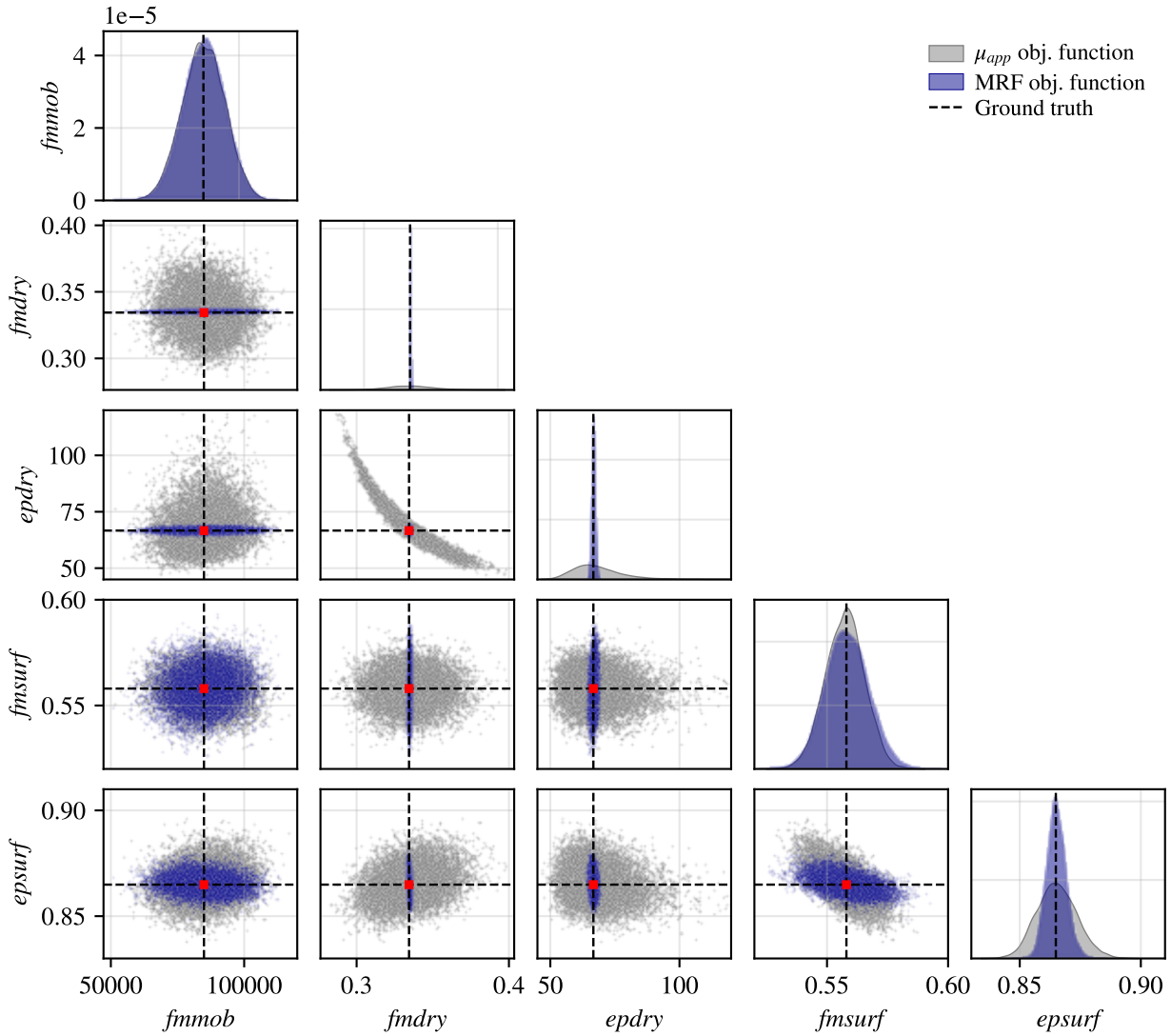

Fig. 7. Comparison of foam parameter estimates from apparent viscosity (gray) and MRF (blue) approaches across 8192 relative permeability realizations.

2013), NMR (Amirmoshiri et al., 2018), or mass balance calculations (Ma et al., 2013), provides parameters less affected by epistemic uncertainties from relative permeability assumptions. Recent studies on uncertainty quantification of relative permeability models (Valdez et al., 2020; Berg et al., 2021, 2024; Ribeiro et al., 2024) have shown that these uncertainties can substantially affect production factors. Therefore, in scenarios where relative permeabilities are highly uncertain, the direct measurement of water saturation in the MRF approach also provides an advantage for estimating dry-out parameters, which are highly sensitive to water saturation, reducing uncertainty propagation.

The MRF approach becomes particularly relevant when considering more complex relative permeability models, such as LET (Lomeland et al., 2005), which include additional parameters for endpoint curvature and transition behavior. Assumptions regarding the estimated values for the relative permeability parameters enable the foam parameter estimation to adjust to the studied dataset and indicate a best estimation set, although it does not accurately represent the actual mobility reduction provided by foam (see Fig. 5 and Tables 3 and 4).

The MRF approach circumvents this mathematical limitation by relying solely on the observed pressure drop and saturation for core flooding experiments (with and without foam). This flexibility sets the estimation of relative permeability as a subsequent step or even a possibility to estimate together with the foam parameters. It avoids bias from functional form assumptions and enables hypothesis testing during the parameter estimation procedure, such as the variation in the residual saturations due to the presence of foam (Mehrabi et al., 2022).

6.2 MRF definition

Beyond the parameter fitting capability, the lack of standardized definitions for experimental MRF (Rosman and Kam, 2009; Simjoo et al., 2013; Sri-Hanamertani et al., 2021), see also the works by AlYousef et al. (2023); Bello et al. (2023);

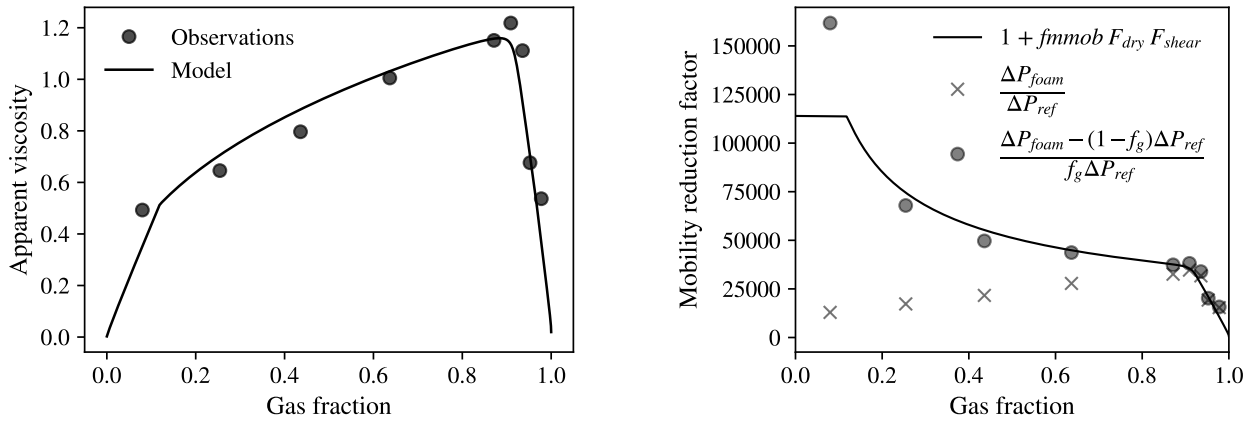

Fig. 8. MRF approach validation on data from Kapetas et al. (2016) with active F_{shear} effects showing good agreement between calculated and theoretical values.

Jia et al. (2024), creates challenges for data interpretation and cross-study comparisons. This inconsistency in experimental protocols produces MRF values that, while sharing nomenclature with the implicit-texture model parameter, represent fundamentally different physical quantities (see Fig. 1). Different experimental MRF definitions (involving reference conditions such as continuous brine injection, continuous gas injection, or water-gas co-injection) yield values that cannot be directly compared or converted into implicit-texture foam parameters without additional data. Without standardization, the same foam system characterized in different laboratories produces MRF values that represent distinct physical quantities despite identical nomenclature.

Although this study focuses exclusively on the effects of surfactant concentration and water saturation, the MRF approach is capable of capturing other foam behaviors, such as shear-thinning effects. However, fitting parameters associated with these additional behaviors would require further data, which have been simplified in the present analysis to consider only dry-out and surfactant effects. For instance, fitting the F_{shear} function from single injection velocity experiments faces identifiability challenges (de Moura Ribeiro et al., 2025).

To further demonstrate the applicability of the proposed MRF expression, an additional analysis using the experimental data provided by Kapetas et al. (2016) was presented. Fig. 8 illustrates the MRF values using the proposed expression for the experimental data of the foam-quality scan presented by Kapetas et al. (2016), along with the fitted parameters from Valdez et al. (2022a) used to simulate both the reference pressure drop and the corresponding ground-truth function. This demonstrates that Eq. (17) remains applicable to other foam physics, such as the non-Newtonian behavior, and may also extend to additional contexts, as long as saturation matching between the reference and foam experiments is preserved.

6.3 Injected surfactant concentrations

Including F_{surf} in the model while using data from a single surfactant concentration may result in identifiability issues. The optimization cannot distinguish between the reference foam strength (*fmmob*) and the concentration-dependent scaling, leading to parameter correlation and non-unique parameters. This coupling manifests as flattened profile likelihood curves or oscillations for both *fmmob* and surfactant parameters. To illustrate this behavior, the profile likelihood analysis was conducted using data from increasing surfactant concentrations (Fig. 9). The results suggest that the non-identifiability cases observed in Fig. 9 (corresponding to the first three cases) arise because the experimental procedure lacks the necessary variation in surfactant concentrations to properly constrain the F_{surf} terms. This issue is due to the absence of data, rather than the estimation method used, whether the proposed MRF approach or the traditional μ_{app} approach. Particularly, in the case examined, at least three surfactant concentrations are needed to prevent identifiability issues, as shown in the bottom panel.

6.4 Translation to field scale

Although upscaling introduces additional complexities, such as heterogeneity and gravitational effects, robust laboratory-scale characterization is the fundamental basis for reliable field models. Field implementation typically employs history matching to refine laboratory-derived parameters using early production data (Alcorn et al., 2022; Sæle et al., 2022). As shown in Table 3, the proposed MRF approach yields lower estimation errors for critical foam parameters, particularly *fmmob*, *fmdry*, and *epdry*, compared to the conventional μ_{app} approach. These parameters control the foam strength and the dry-out behavior, which are essential for predicting foam propagation and stability in reservoirs. Reduced uncertainties in these parameters lead to more accurate field-scale predictions of foam performance, including sweep efficiency and oil recovery. In contrast, the μ_{app} approach introduces larger errors that propagate to field models, potentially resulting in suboptimal foam application designs and economic outcomes. Consequently, uncertainties originating from core-flooding parameter estimation are inevitably transferred to field-scale simulations (Sharma et al., 2020; de Moura Ribeiro et al., 2025).

Biased parameter estimations from uncertain lab estimates either propagate to field predictions or are compensated

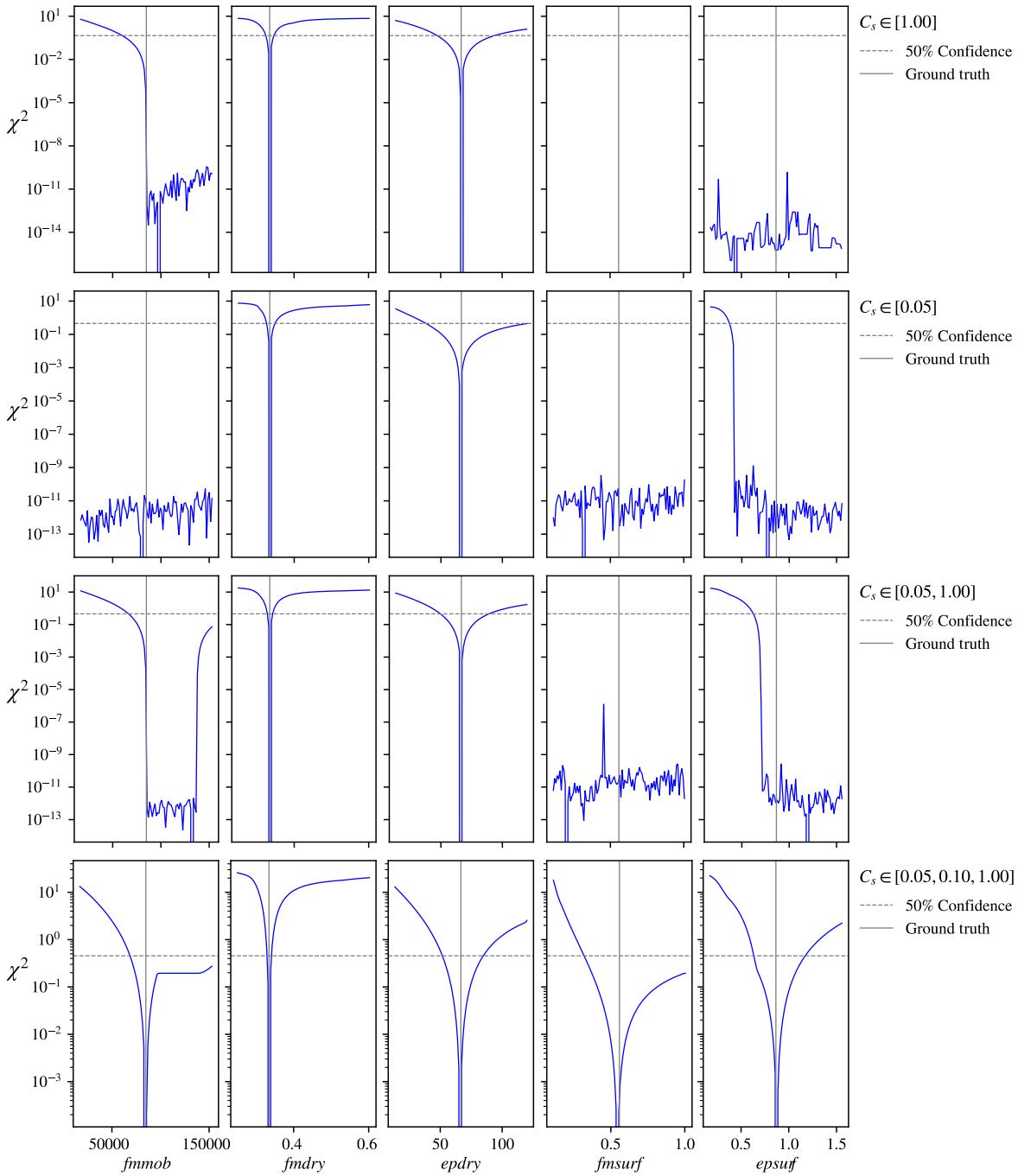

Fig. 9. Profile likelihood analysis showing parameter identifiability improvement with increasing surfactant concentration data points.

through adjustments to reservoir properties during history matching. This misattribution obscures uncertainty sources and reduces physical consistency in forecasts. While this work does not address upscaling or field-scale translation, it strengthens the core-scale characterization essential for field-level modeling.

6.5 Applicability and limitations

The proposed MRF method requires saturation monitoring and a no-foam reference experiment at matching saturations, which may not be feasible in all laboratory settings. In summary, the choice between methods for foam parameter estimation should consider: (1) When relative permeability is well-characterized (low uncertainty), both methods are applicable, though MRF typically provides lower uncertainty due to its circumvention of relative permeability assumptions; (2) when relative permeability is highly uncertain, MRF is preferred; (3) when saturation monitoring is unavailable, the traditional μ_{app} method may be the only option. In addition, one can note that if relative permeability models, such as the LET model, are to be employed, the MRF method remains the preferred choice, since inverting the LET model is not straightforward. The

decision should balance experimental capabilities, required accuracy, and the intended application, as foam parameter estimation is critical for accurate field-scale predictions, where the reliability of parameters significantly impacts forecasts.

7. Conclusions

This study presented an alternative approach for foam parameter estimation in implicit-texture models, which is based on the definition of an alternative MRF expression. The proposed approach introduces the foam quality f_g value into the MRF formula to circumvent the need for relative permeability functions assumption during the estimation of foam parameters. The derived expression provides a standardized metric for comparing foam strength across experiments and laboratories, and serves as an alternative method for parameter estimation.

The LET relative permeability functions were employed with the foam implicit-texture model implemented in CMG-STARS to generate the data and validate the approach capacity to circumvent model assumptions. The analysis of parameter identifiability showed that both the surfactant-related parameters and the dry-out parameters can be reliably estimated using the proposed formulation. Both approaches studied require conducting foam quality scan experiments at a sufficient range of injected concentrations to prevent issues with parameter identifiability.

The MRF formulation provides direct physical interpretability and facilitates meaningful comparisons between foam characterization studies conducted under different experimental conditions. Moreover, uncertainty quantification revealed that the MRF approach enabled more robust parameter estimation by consistently producing lower parameter estimation variances compared to the apparent viscosity approach, particularly for the dry-out parameters *fmdry* and *epdry*. This reduction in uncertainty propagation represents a significant advantage for experimental characterization of foam behavior.

Acknowledgements

The authors gratefully acknowledge support from Shell Brasil through the project “Avançando na modelagem matemática e computacional para apoiar a implementaç ao da tecnologia ‘Foam-assisted WAG’ em reservatórios do Pré-sal” (ANP 23518-4) at UFJF and the strategic importance of the support given by ANP through the R&D levy regulation. G. Chapiro was supported in part by CNPq grants 306970/2022-8, 409718/2024-6, and FAPEMIG grant APQ-00206-24. The authors were supported in part by CAPES (Nos. 88881.708850/2022-01 and 88881.691780/2022-01).

Conflict of interest

The authors declare no competing interest.

References

Alcorn, Z. P., Sæle, A., Karakas, M., et al. Unsteady-state CO_2 foam generation and propagation: Laboratory and field insights. Energies, 2022, 15(18): 6551.

AlYousef, Z., Gizzatov, A., AlMatouq, H., et al. Assessment of foam generation and stabilization in the presence of crude oil using a microfluidics system. Journal of Petroleum Exploration and Production Technology, 2023, 13(4): 1155-1162.

Amirmoshiri, M., Zeng, Y., Chen, Z., et al. Probing the effect of oil type and saturation on foam flow in porous media: Core-flooding and nuclear magnetic resonance (NMR) imaging. Energy & Fuels, 2018, 32(11): 11177-11189.

Bello, A., Ivanova, A., Rodionov, A., et al. An experimental study of high-pressure microscopy and enhanced oil recovery with nanoparticle-stabilised foams in carbonate oil reservoir. Energies, 2023, 16(13): 5120.

Berg, S., Dijk, H., Unsal, E., et al. Simultaneous determination of relative permeability and capillary pressure from an unsteady-state core flooding experiment? Computers and Geotechnics, 2024, 168: 106091.

Berg, S., Unsal, E., Dijk, H. Sensitivity and uncertainty analysis for parameterization of multiphase flow models. Transport in Porous Media, 2021, 140: 27-57.

Bernard, G. G., Jacobs, W. L. Effect of foam on trapped gas saturation and on permeability of porous media to water. Society of Petroleum Engineers Journal, 1965, 5(4): 295-300.

Bond, D. C., Holbrook, O. C. Gas drive oil recovery process. US2866507, 1956.

Brooks, R. H., Corey, A. T. Hydraulic properties of porous media and their relation to drainage design. Transactions of the ASAE, 1964, 7: 26-28.

Cavalcante Filho, J. S. A., Delshad, M., Sepehrnoori, K. Estimation of foam-flow parameters for local equilibrium methods by use of steady-state flow experiments and optimization algorithms. SPE Reservoir Evaluation & Engineering, 2017, 21(1): 160-173.

Chang, S. H., Grigg, R. Foam displacement modeling in CO_2 flooding processes. Paper SPE 35401 Presented at SPE/DOE Improved Oil Recovery Symposium, Tulsa, Oklahoma, 21-24 April, 1996.

de Miranda, G. B., dos Santos, R. W., Chapiro, G., et al. Uncertainty quantification on foam modeling: The interplay of relative permeability and implicit-texture foam parameters. Transport in Porous Media, 2024, 152: 8.

de Miranda, G. B., Ribeiro, L. S., Façanha, J. M. D. F., et al. Characterization of foam-assisted water-gas flow via inverse uncertainty quantification techniques. Paper Presented at Computational Science – ICCS 2022, London, UK, 21-23 June, 2022.

de Moura Ribeiro, A., Lopes, L. F., Rocha, B. M., et al. Quantifying experimental impacts on non-newtonian foam characterization for flow modeling in porous media: Insights from foam-quality and flow rate scan experiments. Water Resources Research, 2025, 61(9): e2024WR039536.

Eftekhari, A. A., Farajzadeh, R. Effect of foam on liquid phase mobility in porous media. Scientific Reports, 2017, 7(1): 43870.

Farajzadeh, R., Lotfollahi, M., Eftekhari, A. A., et al. Effect of permeability on foam-model parameters and the limiting capillary pressure. Paper cp-445-00044 Presented at IOR 2015 - 18th European Symposium on Improved Oil Recovery, Dresden, Germany, 14-16 April, 2015.

Hematpur, H., Hosseini, S., Mahmood, S. M., et al. A new approach to foam flooding modelling with novel parameter estimation techniques. Scientific Reports, 2025, 15: 22829.

Iman, R. L., Conover, W. J. A distribution-free approach to inducing rank correlation among input variables. Communications in Statistics - Simulation and Computation, 1982, 11(3): 311-334.

Jia, H., Yu, H., Wang, T., et al. Investigation of non-chemical CO_2 microbubbles for enhanced oil recovery and carbon sequestration in heterogeneous porous media. Geoenergy Science and Engineering, 2024, 242: 213229.

Jones, S. A., Laskaris, G., Vincent-Bonnieu, S., et al. Effect of surfactant concentration on foam: From coreflood experiments to implicit-texture foam-model parameters. Journal of Industrial and Engineering Chemistry, 2016, 37: 268-276.

Kahrobaei, S., Farajzadeh, R. Insights into effects of surfactant concentration on foam behavior in porous media. Energy & Fuels, 2019, 33(2): 822-829.

Kapetas, L., Vincent-Bonnieu, S., Danelis, S., et al. Effect of temperature on foam flow in porous media. Journal of Industrial and Engineering Chemistry, 2016, 36: 229-237.

Kovscek, A. R., Radke, C. J. Fundamentals of foam transport in porous media. California, Lawrence Berkeley Laboratory, 1994.

Lake, L. W. Enhanced Oil Recovery. Prentice Hall Inc., Old Tappan, USA, 1988.

Lomeland, F., Ebeltoft, E., Thomas, W. H. A new versatile relative permeability correlation. Paper Presented at International symposium of the society of core analysts, Toronto, Canada, 21-25 August, 2005.

Lotfollahi, M., Farajzadeh, R., Delshad, M., et al. Comparison of implicit-texture and population-balance foam models. Journal of Natural Gas Science and Engineering, 2016, 31: 184-197.

Ma, K., Lopez-Salinas, J. L., Puerto, M. C., et al. Estimation of parameters for the simulation of foam flow through porous media. part 1: The dry-out effect. Energy & Fuels, 2013, 27(5): 2363-2375.

Ma, K., Ren, G., Mateen, K., et al. Literature review of modeling techniques for foam flow through porous media. Paper SPE 169104 Presented at SPE Improved Oil Recovery Symposium, Tulsa, Oklahoma, USA, 12-16 April, 2014.

Ma, K., Ren, G., Mateen, K., et al. Modeling techniques for foam flow in porous media. SPE Journal, 2015, 20(3): 453-470.

Mehrabi, M., Sepehrnoori, K., Delshad, M. Displacement theory of low-tension gas flooding. Transport in Porous Media, 2022, 142(3): 475-491.

Mohammadi, S., Collins, J., Coombe, D. A. Field application and simulation of foam for gas diversion. Paper cp-107-00055 Presented at IOR 1995 - 8th European Symposium on Improved Oil Recovery, Vienna, Austria, 15-17 May, 1995.

Osterloh, W. T., Jante, M. J. Effects of gas and liquid velocity on steady-state foam flow at high temperature. Paper SPE 24179 Presented at SPE/DOE Enhanced Oil Recovery Symposium, Tulsa, Oklahoma, 22-24 April, 1992.

Price, K. V. Differential Evolution, in Handbook of Optimization: From Classical to Modern Approach, edited by I. Zelinka, V. Snášel, A. Abraham, Springer, Berlin, Heidelberg, pp. 187-214, 2013.

Raue, A., Kreutz, C., Maiwald, T., et al. Structural and practical identifiability analysis of partially observed dynamical models by exploiting the profile likelihood. Bioinformatics, 2009, 25(15): 1923-1929.

Ribeiro, L. S., Miranda, G. B., Rocha, B. M., et al. On the identifiability of relative permeability and foam displacement parameters in porous media flow. Water Resources Research, 2024, 60(3): e2023WR036751.

Rosman, A., Kam, S. I. Modeling foam-diversion process using three-phase fractional flow analysis in a layered system. Energy Sources, Part A: Recovery, Utilization, and Environmental Effects, 2009, 31(11): 936-955.

Rossen, W. R. Foams in Enhanced Oil Recovery. Routledge, London, UK, 1996.

Sæle, A., Graue, A., Alcorn, Z. P. Unsteady-state CO_2 foam injection for increasing enhanced oil recovery and carbon storage potential. Advances in Geo-Energy Research, 2022, 6(6): 472-481.

Shafiei, M., Kazemzadeh, Y., Escrochi, M., et al. A comprehensive review direct methods to overcome the limitations of gas injection during the eor process. Scientific Reports, 2024, 14(1): 7468.

Sharma, M., Alcorn, Z. P., Fredriksen, S. B., et al. Model calibration for forecasting CO_2-foam enhanced oil recovery field pilot performance in a carbonate reservoir. Petroleum Geoscience, 2020, 26(1): 141-149.

Simjoo, M., Dong, Y., Andrianov, A., et al. Novel insight into foam mobility control. SPE Journal, 2013, 18(3): 416-427.

Sri-Hanamertani, A., Saraji, S., Piri, M. The effects of *In-Situ* emulsion formation and superficial velocity on foam performance in high-permeability porous media. Fuel, 2021, 306: 121575.

STARS, C. Stars user guide, 2017.

Storn, R., Price, K. Differential evolution – A simple and efficient heuristic for global optimization over continuous spaces. Journal of Global Optimization, 1997, 11(4): 341-359.

Tripathi, R., Alcorn, Z. P., Graue, A., et al. Combination of non-ionic and cationic surfactants in generating stable CO_2 foam for enhanced oil recovery and carbon storage. Advances in Geo-Energy Research, 2024, 13(1): 42-55.

Valdez, A. R., Rocha, B. M., Chapiro, G., et al. Uncertainty quantification and sensitivity analysis for relative per-

meability models of two-phase flow in porous media. Journal of Petroleum Science and Engineering, 2020, 192: 107297.

Valdez, A. R., Rocha, B. M., Chapiro, G., et al. Assessing uncertainties and identifiability of foam displacement models employing different objective functions for parameter estimation. Journal of Petroleum Science and Engineering, 2022a, 214: 110551.

Valdez, A. R., Rocha, B. M., Façanha, J. M., et al. Foam-assisted water-gas flow parameters: From core-flood experiment to uncertainty quantification and sensitivity analysis. Transport in Porous Media, 2022b, 144: 189-209.

Vicard, A., Atteia, O., Bertin, H., et al. Estimation of local equilibrium foam model parameters as functions of the foam quality and the total superficial velocity. ACS Omega, 2022, 7(20): 16866-16876.

Vieira, R. A. M., Dos Santos, S. S. F., Do Nascimento, L. P. T., et al. Experimental characterization to support a fawag project in an offshore pre-salt field. Paper SPE 218195 Presented at SPE Improved Oil Recovery Conference, Tulsa, Oklahoma, USA, 22-25 April, 2024.

Wang, Z., Li, S., Xu, Z., et al. Advances and challenges in foam stability: Applications, mechanisms, and future directions. Capillarity, 2025, 15(3): 58-73.

Zavala, R. Q., Lozano, L. F., Chapiro, G. Traveling wave solutions describing the foam flow in porous media for low surfactant concentration. Computational Geosciences, 2024, 28(2): 323-340.

Zeng, Y., Muthuswamy, A., Ma, K., et al. Insights on foam transport from a texture-implicit local-equilibrium model with an improved parameter estimation algorithm. Industrial & Engineering Chemistry Research, 2016, 55(28): 7819-7829.